

Kondo versus magnetic coupling of cobalt dimers in a Cu–O (2×1) reconstruction

This article has been downloaded from IOPscience. Please scroll down to see the full text article.

2010 J. Phys.: Condens. Matter 22 222202

(<http://iopscience.iop.org/0953-8984/22/22/222202>)

View [the table of contents for this issue](#), or go to the [journal homepage](#) for more

Download details:

IP Address: 129.252.86.83

The article was downloaded on 30/05/2010 at 08:48

Please note that [terms and conditions apply](#).

FAST TRACK COMMUNICATION

Kondo versus magnetic coupling of cobalt dimers in a Cu–O (2×1) reconstruction

Andreas Gumbusch¹, Giovanni Barcaro², Mike G Ramsey¹,
Svetlozar Surnev¹, Alessandro Fortunelli^{2,3} and Falko P Netzer^{1,3}

¹ Institute of Physics, Surface and Interface Physics, Karl-Franzens University Graz,
A-8010 Graz, Austria

² Molecular Modeling Laboratory, Istituto per i Processi Chimico-Fisici (IPCF), CNR,
I-56124 Pisa, Italy

E-mail: fortunelli@ipcf.cnr.it and falko.netzer@uni-graz.at


Received 24 April 2010, in final form 30 April 2010

Published 20 May 2010

Online at stacks.iop.org/JPhysCM/22/222202

Abstract

Co atoms and dimers embedded in a Cu(110)(2×1)–O surface oxide are investigated via low-temperature STM/STS experiments and first-principles simulations. It is found that Co dimers incorporated into adjacent rows of the Cu(110)(2×1)–O reconstruction show Kondo resonances decoupled from each other, whereas they are antiferromagnetically coupled (and do not exhibit a Kondo effect) when they are aligned on the same row. This shows that it is possible to decouple single carriers of the Kondo effect via a proper choice of the adsorption and host geometry. It is also shown that an oxidic environment presents features remarkably different from those of pure metal substrates.

 Online supplementary data available from stacks.iop.org/JPhysCM/22/222202/mmedia

(Some figures in this article are in colour only in the electronic version)

In the last 12 years, modern developments in surface science have allowed researchers to demonstrate the Kondo effect, a previously well-known and widely studied phenomenon in condensed-matter physics [1–3], on novel classes of materials and to characterize its features with unprecedented accuracy [4–6]. This combined very well with the theme of collective many-body interactions that are at the basis of the surface Kondo effect and make it an ideal testing ground for understanding and controlling quantum phenomena that are expected to dominate as the limits of miniaturization are approached in nanotechnological devices. Spin-flip scattering processes between the electrons of the magnetic species and the conduction band electrons of the host produce a non-magnetic correlated electronic quantum state, whose signature in scanning tunneling spectroscopy (STS) is a resonance positioned in close proximity to the Fermi level [7]. The resonance in STS has a Fano-like appearance [8], as it arises from the interference of two competing scattering

channels. An analysis of its features thus provides access to information on the electronic interactions between the host and the impurity which would be very difficult to obtain otherwise. The length scale of these interactions, the so-called Kondo screening length, in which the impurity spin is screened, is estimated to extend for tens of nanometers (10–100 nm), involving 10^5 – 10^8 atoms [9]. Although the basic physics of the Kondo effect has been known for a long time [1], a quantitative understanding is needed if control on, and design of, real devices is to be achieved. Finding new, atomically characterized examples is crucial in this respect, as surprises and counterintuitive trends have been shown to occur [10, 11], in particular by enlarging the set of well-defined systems from the original magnetic metal adatoms on single-crystal metal surfaces to more exotic substrates, but at the same time closer to real-world applications, such as surface or ultrathin oxides and nitrides [7]. In this perspective, it is especially important that not only the principles governing the impurity/host but also the interaction among single scatterers need to be fully clarified as functions of the chemistry and

³ Authors to whom any correspondence should be addressed.

geometry of adsorption, another important theme in current nanoscience [12].

In the present work, this research plan is pursued by investigating via STM/STS Co adatoms on, and Co atoms and dimers embedded in, a Cu(110)(2 × 1)-O surface oxide. Co adatoms on the bare Cu(110) surface have been studied in a previous work [10], showing that they exhibit a Kondo resonance with a peak-like instead of a dip-like Fano shape, as observed for Co adatoms on other Cu surfaces [13]. The main finding here is that pairs of first-neighbor Co atoms incorporated into adjacent parallel rows of the Cu(110)(2 × 1)-O surface show Kondo resonances essentially decoupled from each other, whereas they are antiferromagnetically coupled (and thus do not exhibit any Kondo effect) when they are aligned in the same Cu-O row. In other words, we find that Co first-neighbor dimers can exhibit a completely different magnetic behavior depending on the geometry of adsorption, despite the fact that they lie at comparable close-contact distances. These results, which are in keeping with the predictions of density functional (DF) simulations, indicate first of all that—despite the intrinsically long-range character of the Kondo phenomenon—it is possible to decouple single carriers of the Kondo quantum effect from each other via a proper choice of the interaction geometry, with promising implications in terms of technological devices. Additionally, it is shown that an oxidic environment (closer to real-world applications) presents features somewhat different from pure metal systems, not only because the oxygen atoms can mediate the interactions among impurity atoms, in one present case switching from ferromagnetic to antiferromagnetic coupling, but also because they influence appreciably their charge and spin state, and thus ultimately their Kondo response. This is supported by arguments based on theoretically derived quantities such as the weighted coordination number, the 3d population and the local density of states (LDOS) at the Fermi level.

The STM/STS experiments have been carried out in a three-chamber low-temperature STM system (Creteac, Germany) in an ultrahigh vacuum (UHV) with a base pressure of $\sim 5 \times 10^{-11}$ mbar, operated at a measurement temperature of ~ 5 – 6 K in the liquid He STM cryostat stage as described previously [10]. The Cu(110)(2 × 1)-O reconstruction was prepared by exposing the clean Cu(110) surface to 1 L O₂ (1 Langmuir (L) = 1×10^{-6} Torr s) at a sample temperature of 600 K followed by annealing in UHV. Further details of the experiment and the preparation of the Cu(110)2 × 1-O surface including the deposition of Co impurity atoms are described in the supplementary material (available at stacks.iop.org/JPhysCM/22/222202/mmedia).

DF calculations were performed using the PWscf (plane-wave self-consistent field) computational code [14], employing ultrasoft pseudopotentials [15] and the PBE exchange–correlation functional [16] within a DF + U approach [17] with a value of U for the Co species equal to 3.0 eV. A DF + U approach is known to produce more accurate results than a pure DF one for Co in oxidic environments [17]. It can be noted that we use a conservative value of $U = 3.0$ eV, which lies at the lower edge of the range usually considered

in the literature [18]. The calculations on the non-oxidized systems were also performed using a standard DF approach, finding completely analogous results. Other computational details can be found in the supplementary material (available at stacks.iop.org/JPhysCM/22/222202/mmedia).

Figure 1 contains atom-resolved constant-current topographic STM images of Co atoms on Cu(110)(2 × 1)-O surfaces in different configurations and chemical environments (leftmost side) together with corresponding geometrical models (middle) and STS spectra taken from the top of the Co atoms (rightmost side). Figure 1(a) shows a single Co atom *adsorbed* on the Cu-O surface in between the Cu-O rows (indicated by the green lines), imaged as a bright protrusion in STM: a-Co/Cu(110)-O; the corresponding STS spectrum displays the Kondo resonance as a dip feature somewhat above the Fermi energy ($E_F = 0$ V sample bias). A single Co atom *embedded* into the Cu-O row substituting a Cu atom is clearly visible in bright contrast in the STM image of figure 1(b): e-Co/Cu(110)-O, and the STS spectrum of the embedded monomer shows a dip-like Kondo resonance feature, but with modifications in energy position and width. The STM image of figure 1(c) shows an embedded Co dimer along the $[1\bar{1}0]$ direction: e-Co₂ $[1\bar{1}0]$ /Cu(110)-O, and the corresponding STS spectrum is found to be virtually identical to that of the embedded monomer in figure 1(b). In figure 1(d) an embedded Co dimer along the $[001]$ direction is imaged: e-Co₂ $[100]$ /Cu(110)-O; in the associated STS spectrum, however, the Kondo resonance around the Fermi energy is quenched.

As mentioned above, the form of the Kondo resonance in the STS spectra may be described by a Fano line function [7, 8]:

$$(dI/dV)(V)\alpha(q + \varepsilon)^2/(1 + \varepsilon^2) + c \quad (1)$$

with the normalized energy $\varepsilon = (eV - \delta)/\Gamma$ and a constant c . The parameters q , δ and Γ are fitting parameters for the experimental data and signify the asymmetry parameter q , the energy shift δ of the Kondo resonance from zero bias (i.e. E_F) and the half-width of the feature at half-maximum Γ , which is related to the characteristic Kondo temperature $T_K = \Gamma/k_B$ (where k_B is the Boltzmann constant). Figure 2 displays the Fano fits of the STS data for a Co atom *adsorbed* on the Cu(110)(2 × 1)-O reconstruction (panel (a)) and for a Co atom *embedded* into the Cu-O rows (panel (b)). The data in figure 2 have been background-corrected before fitting, i.e. the corresponding STS spectra of the bare substrates, recorded in the same experimental run with strictly the same tip conditions, have been subtracted directly without normalization from the raw spectra (such as shown in figure 1). The average Fano fitting parameters obtained from the analysis of a large dataset are given in table 1, which also contains data of Co adsorbed on the clean Cu(110) surface from our previous work [10] and of Co/Cu(100) and Co/Cu(111) from [13].

DF calculations were performed on systems composed of Co atoms in different sites of Cu surfaces: a-Co/Cu(110)-O, e-Co/Cu(110)-O, e-Co₂ $[1\bar{1}0]$ /Cu(110)-O and e-Co₂ $[100]$ /Cu(110)-O, considered in the present work, and also Co/Cu(110), Co/Cu(111) and Co/Cu(100), on which STS

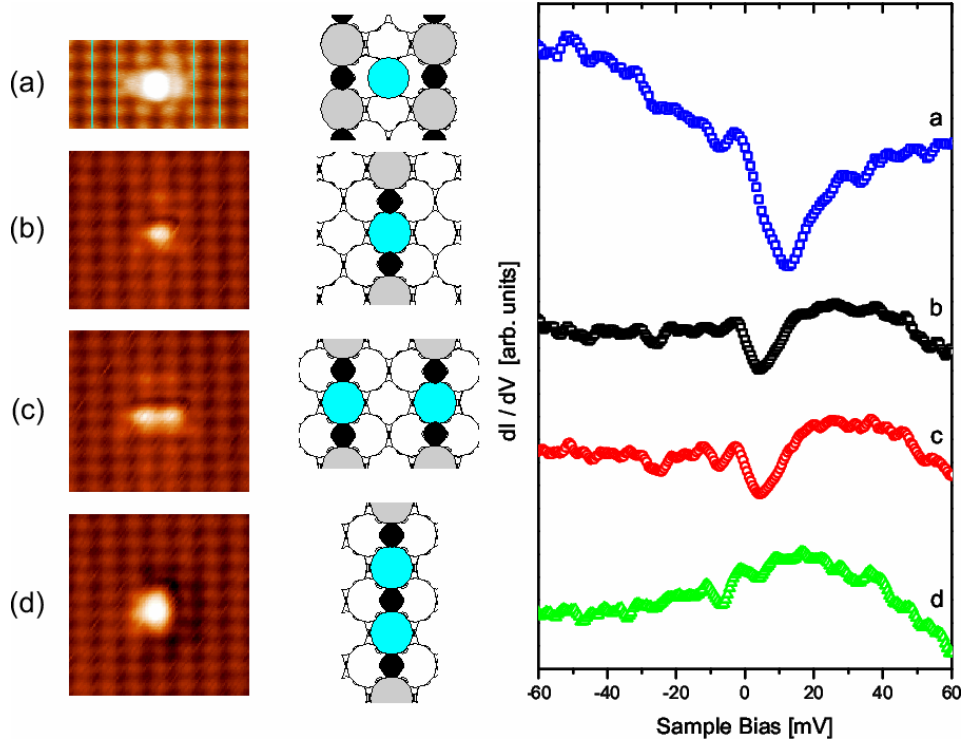


Figure 1. Topographic STM images (leftmost side), schematic geometrical models (middle) and differential conductance STS spectra (rightmost side, dI/dV versus V): (a) single Co adatom adsorbed on Cu(110) 2×1 -O (a-Co/Cu(110)-O), Cu-O rows along the [001] direction are indicated by lines in the STM image (STM image parameters: $36 \times 38 \text{ \AA}^2$; sample bias: 1 V; tunneling current: 0.5 nA); (b) Co monomer embedded in the Cu(110) 2×1 -O layer (e-Co/Cu(110)-O), ($36 \times 32 \text{ \AA}^2$; -10 mV; 1 nA); (c) Co dimer embedded in Cu(110) 2×1 -O along $[1\bar{1}0]$ (e-Co₂[$1\bar{1}0$]/Cu(110)-O), ($36 \times 33 \text{ \AA}^2$; -10 mV; 1 nA); (d) Co dimer embedded in Cu(110) 2×1 -O along [001] (e-Co₂[100]/Cu(110)-O), ($36 \times 36 \text{ \AA}^2$; -10 mV; 1 nA).

Table 1. Number of spin majority ($n_{d\alpha}$) and spin minority ($n_{d\beta}$) electrons on Co d -orbitals (the corresponding values for s -orbitals, $n_{s\alpha}$ and $n_{s\beta}$, are given in parentheses); spin polarization (SP = $n_{d\alpha} - n_{d\beta}$) and total population ($n_d = n_{d\alpha} + n_{d\beta}$) in the d space; distances (r_{ij} , in \AA) of Cu close-neighbors from Co atoms; coordination number (CN) calculated according to equation (2); average Kondo temperature T_K (in Kelvin) and average Fano fitting parameters δ , Γ and q . δ and Γ are in meV.

System	$n_{d\alpha}$ ($n_{s\alpha}$)	$n_{d\beta}$ ($n_{s\beta}$)	SP	n_d	r_{ij} (\AA)	CN	T_K (K)	δ (meV)	Γ (meV)	q
Co/Cu(110)	4.95 (0.58)	2.87 (0.44)	2.08	0.82	$2.24 + 4 \times 2.45$	0.44	125 ± 30	6.9 ± 2.1	10.8 ± 2.6	Peak
a-Co/Cu(110)-O	4.78 (0.35)	2.96 (0.38)	1.82	0.74	$2 \times 2.53 + 4 \times 2.89$	0.38	93 ± 8	8.9 ± 3.0	8.0 ± 0.7	Dip
Co/Cu(100)	4.94 (0.54)	2.97 (0.46)	1.97	0.91	4×2.44	0.35	88 ± 4	-1.3 ± 0.4	7.6 ± 0.3	Dip
Co/Cu(111)	4.96 (0.58)	2.94 (0.44)	2.02	0.90	3×2.38	0.28	54 ± 2	1.8 ± 0.6	4.9 ± 0.2	Dip
e-Co/Cu(110)-O	4.74 (0.32)	3.01 (0.34)	1.75	0.75	5×2.61	0.36	57 ± 4	3.3 ± 1.3	4.9 ± 0.3	Dip

experiments have been conducted [10, 19] and which will be used for comparison purposes. DF theory being essentially a mean-field approach, it cannot capture the complex many-body physics of the Kondo phenomenon. Several approaches have been proposed in the literature to link first-principles calculations to predictions of the shape and position of the Kondo resonance, see, for example, [20–27], although many rely in one way or another on qualitative fits or on the use of empirical parameters, whose values are fixed on the

basis of physical intuition or to match experimental data or first-principles quantities. A really quantitative and general understanding of the Kondo effect has not yet been achieved. In this context, electronic structure DF calculations can provide a framework in which simplified models operate and give information useful to discuss experimental data.

The geometries of Co atoms and dimers on/in the oxidized Cu(110) surface layer are schematically depicted in figures 1(a)–(d). The distances between the Co atom and its

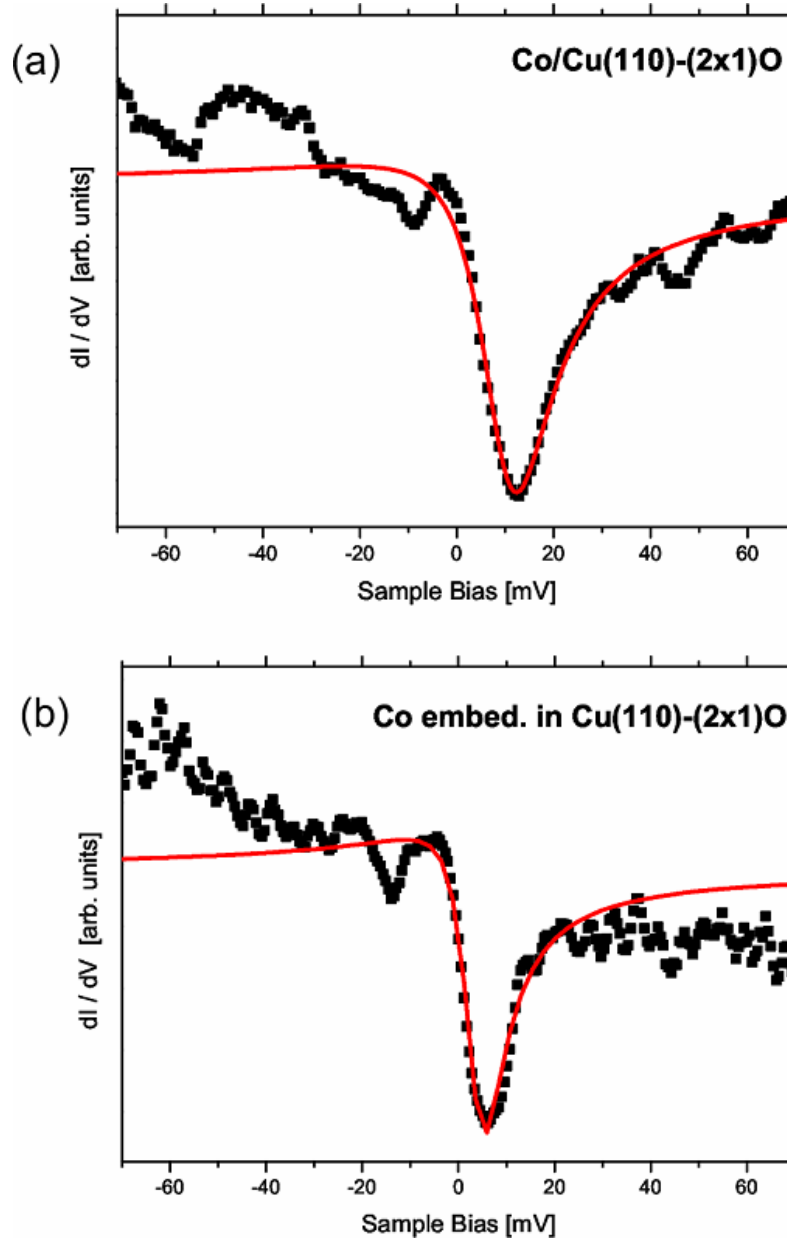


Figure 2. Fano lineshape fits to the STS spectra of Co monomers: (a) adsorbed on Cu(110) 2×1 -O and (b) embedded in Cu(110) 2×1 -O. The corresponding fitting parameters are given in table 1.

nearest-neighbor Cu atoms (r_{ij}) as derived from DF energy minimizations are reported in table 1 for all the systems considered here, together with the average number of electrons in the Co 3d and 3s majority ($n_{d\alpha}$ and $n_{s\alpha}$, respectively) and minority ($n_{d\beta}$ and $n_{s\beta}$, respectively) spin bands, evaluated via a Lowdin projection of the wavefunction, and the experimentally derived values of the Kondo temperature (T_K), the position of the Kondo resonance with respect to the Fermi energy (δ) and the asymmetry parameter of the Kondo resonance (q). A few notable differences among the various systems considered here can be drawn from an inspection of table 1, which can be analyzed in detail in comparison with experimental data.

We start by analyzing the Co interaction geometry. From table 1, one can see that both the number and the distances of Cu atoms next to Co vary significantly for the various systems.

This variation can be summarized into a single parameter as the coordination number [13]:

$$CN = \sum_{j^{\text{th}} \text{ Cu neighbor}} \exp(-r_{ij}) \quad (2)$$

where r_{ij} is the distance of the j^{th} Cu neighbor from the Co impurity atom, evaluated from the DF local energy minimizations and reported in table 1. From table 1, one can see that CN varies from a minimum of 0.28 for Co/Cu(111) to a maximum of ≈ 0.44 for Co/Cu(110). In between, we find a group of three systems, namely Cu(100) and the oxidized Cu(110) surfaces, with similar CN values, $CN = 0.35$ – 0.38 . It can be noted that in the oxidized systems Co has 5–6 neighbors, but the increase in the Co–Cu distances reduces the CN value from the maximum realized for the bare Cu(110) surface.

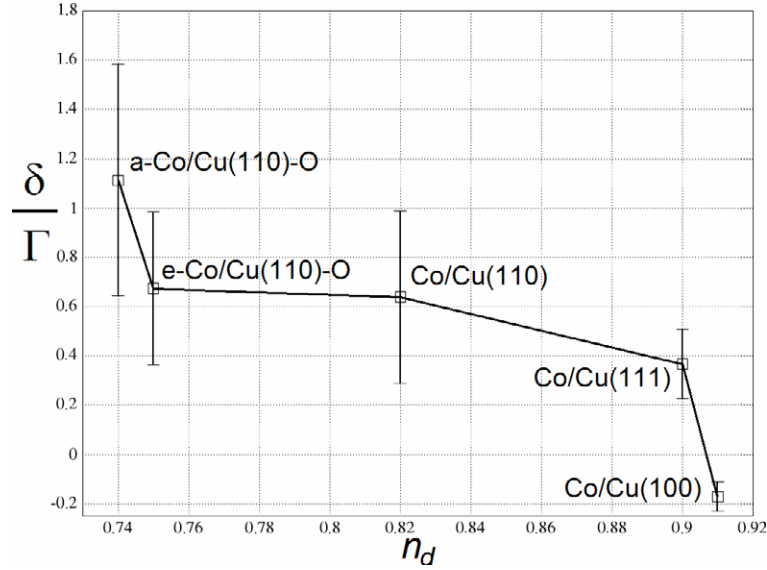


Figure 3. Plot of the position of the Kondo resonance with respect to the Fermi energy divided by its width (δ/Γ) (experimental values from the present work or [13]) as a function of the occupation number of the 3d states, n_d , for the five Co adsorption configurations considered in the present work. n_d is calculated according to equation (4) (see text). Experimental error bars are also shown.

The difference between oxidized and non-oxidized systems is even clearer from an analysis of the atomic populations: $n_{d\alpha}$, $n_{s\alpha}$, $n_{d\beta}$ and $n_{s\beta}$. The atomic configuration of Co, as it emerges from these values, is $3d^8 4s^1$, realized via atomic populations which—very roughly—are: $n_{d\alpha} \approx 5$, $n_{d\beta} \approx 3$, $n_{s\alpha} \approx n_{s\beta} \approx 0.5$. The net spin polarization is therefore around 2, corresponding to two impurity orbitals or a two-channel Kondo system. A more detailed analysis, however, highlights marked differences. First, $(n_{s\alpha} + n_{s\beta}) \approx 1$ and $n_{d\alpha} \approx 5$ for the bare surfaces, whereas $(n_{s\alpha} + n_{s\beta}) \approx 0.66$ – 0.73 and $n_{d\alpha} \approx 4.74$ – 4.78 for the oxidized systems. The Co atom is therefore partially oxidized in the latter cases. Second, the spin polarization in the d space ($n_{d\alpha} - n_{d\beta}$) is ≈ 2 for the bare systems, whereas $(n_{d\alpha} - n_{d\beta})$ is ≈ 1.82 for the adatom on the oxidized (110) surface and even smaller (1.75) for a Co atom embedded in the same surface (the fact that the spin polarization for the oxidized systems is reduced will be used below).

The charge state of the impurity immediately reflects on the position δ of the Kondo resonance. This quantity is, in fact, related to the occupation number n_d of the 3d states of the adatom on the surface by the relation [2]

$$\delta = \Gamma \tan[\pi/2(1 - n_d)]. \quad (3)$$

The average occupation number n_d can be estimated using atomic populations derived via a Lowdin projection of the DF wavefunction (see table 1) as

$$n_d = n_{d\alpha} + n_{d\beta} - 7. \quad (4)$$

In figure 3 the values of the ratio δ/Γ for the five systems under consideration are plotted as a function of n_d . In qualitative agreement with equation (3), the ratio between the Kondo shift δ and the width of the Kondo resonance Γ increases with decreasing occupation number n_d , reaching its maximum

for the a-Cu(110)(2×1)-O system, even though an accurate interpolation is not possible, also due to uncertainties in the δ values and to the approximate values of n_d derived from Lowdin populations.

The Kondo temperature can be discussed along lines similar to those followed in [13, 26, 27], where it has been argued that the coordination number of the adsorption site may be taken as a simple scaling measure of the Kondo temperature, and experimental data on a number of systems have been presented in support of this notion. However, it has also been pointed out that this simple scaling behavior may not be sufficient to describe all the observations on adsorbate cluster and ligand systems [11, 28] and that a more refined picture may be necessary involving detailed electronic structure calculations to reveal the local density of states at the Fermi level. We use the equation (derived in the weak coupling limit of the s-d model [7] via the Schrieffer-Wolff transformation [29, 2])

$$k_B T_K = [(U\Delta)/2]^{1/2} \exp[-\pi/(2U\Delta)|\varepsilon_d||\varepsilon_d + U|] \quad (5)$$

where Δ is the hybridization matrix element that couples the localized state with the continuum of band states as above, U is the on-site Coulomb repulsion and ε_d is the position of the impurity d-level with respect to the Fermi energy. By then, assuming that U and ε_d are roughly constant, linearizing T_K as a function of Δ (which is legitimate as Δ varies in a narrow range), and assuming that Δ , being related to the broadening of the impurity state, is roughly proportional to the coordination number CN [13], we can plot T_K as a function of CN , as shown in figure 4(a). An inspection of this figure immediately reveals that the oxidized systems, e-Co/Cu(110)-O in particular, do not scale properly with CN , in contrast to the linear relationship found for the other systems. This is not unexpected, as the above analysis of

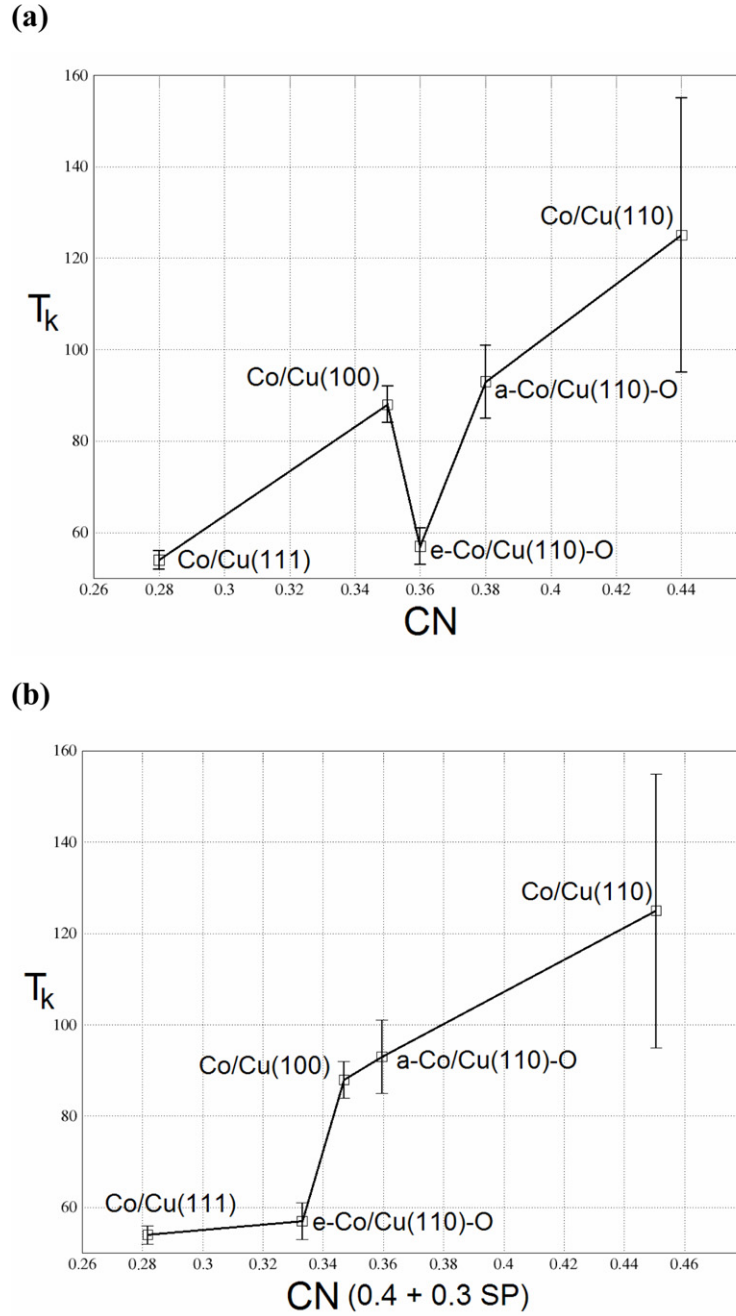


Figure 4. Kondo temperature T_K (experimental values in Kelvin from the present work or [13]) versus standard (a) or corrected (b) coordination number (CN). CN is derived from the present DF calculations for Co atoms on different Cu surfaces. The corrected CN is modulated by the spin polarization (SP) for each system, see equation (6). Experimental error bars are also shown.

the atomic populations already pointed out a clear difference between non-oxidized and oxidized systems, in particular for e-Co/Cu(110)-O. Indeed, it is precisely for these systems that one finds values of the spin polarization appreciably smaller than the value of ~ 2 valid for the bare Cu surfaces. One can try to correct for this effect by multiplying CN by a weighting factor that takes spin polarization into account. We derive this factor from the analysis of [23], where the Kondo response of Fe atoms embedded in fcc Au was studied, and it was found from renormalization group calculations that the Kondo temperature scaled linearly with respect to the spin state of the

Fe atom according to the formula

$$T_K \approx T_K^0 [0.4 + 0.3(n_{d\alpha} - n_{d\beta})] \quad (6)$$

being 0.7 for $S = 1/2$, 1.0 for $S = 1$ and 1.3 for $S = 3/2$ (see figure 3 of [23] in proper units). By correcting the coordination number for the spin polarization weighting factor given by equation (6), the plot of figure 4(b) results, in which a better agreement with linear behavior can be appreciated, despite the heuristic character of the present analysis.

Co 3d-LDOS plots are shown for comparison purposes in figure 1 of the supplementary material (available at

stacks.iop.org/JPhysCM/22/222202/mmedia) for the systems considered here. In passing, we observe that in analogy with [10] a correlation between the density of Co 3d states at the Fermi energy and the shape of the Kondo resonance is found: a low Co d-LDOS at the Fermi energy is associated with a dip-like shape of the Kondo resonance, whereas a high Co d-LDOS at the Fermi energy is associated with a peak-like shape.

The previous analysis shows that an oxidic environment entails appreciable differences with respect to the more thoroughly investigated metal supports, specifically in terms of both the charge and spin state of the impurity atom. Even more striking results are obtained for the dimer configurations—figures 1(c) and (d). First of all, we immediately find a qualitative difference in the magnetic properties of the system between the case in which the two Co atoms are positioned in the same chain, figure 1(d), versus in parallel chains, figure 1(c), i.e. between dimers positioned along the [001] or [1 $\bar{1}$ 0] directions, respectively. Total energy calculations show that in the case that the dimers are along [1 $\bar{1}$ 0] the energy difference between spin configurations in which the Co atoms are ferromagnetically or antiferromagnetically coupled is below numerical accuracy (less than 0.01 eV) and the system resembles a pair of essentially decoupled embedded Co atoms. It is therefore to be expected that the Kondo response of the system will be a superposition of two single-atom contributions, in agreement with experimental observations. This occurs despite the fact that the spin waves induced in the substrate by the two Co impurities interfere with each other, as is visible in figure 2 of the supplementary material (available at stacks.iop.org/JPhysCM/22/222202/mmedia). In contrast, in the case that the dimers are along [001] one finds that this energy difference amounts to 0.18 eV, with the Co atoms antiferromagnetically coupled in the ground state. Also the LDOS of a dimer along the [1 $\bar{1}$ 0] direction (see figure 1 of the supplementary material available at stacks.iop.org/JPhysCM/22/222202/mmedia) is very similar to the single-atom case, whereas it presents appreciable differences for a dimer along the [001] direction. The complete decoupling of close neighbors in the [1 $\bar{1}$ 0]-oriented dimer is particularly surprising. It is known, in fact, that the perturbation produced by the impurity decays slowly with distance in such a way that the cloud of screening electrons extends for tens of nm inside the host [9], and collective phenomena due to long-range interactions among single scatterers have been experimentally demonstrated [12]. Our finding proves that the Kondo phenomenon is extremely sensitive to the geometry of the interaction, an important point when the design of independent scatterers is sought for. As for the [001]-oriented dimer, a Co–Co antiferromagnetic coupling may sound unexpected, as Co is a ferromagnet in the bulk and ferromagnetic coupling has been observed for close pairs of Co atoms [30], whereas antiferromagnetic coupling is only expected for much larger distances [31, 28]. However, in the present case the Co–Co interaction is mediated by an oxygen atom and, even though the oxidation state of Co is only a little higher than that of Co atoms on bare Cu surfaces, the system in some respects resembles a CoO oxide, which is an antiferromagnet in the

bulk [18]. This is consistent with the Goodenough–Kanamori rules [32, 33] which also predict antiferromagnetic coupling in the given geometry. The energy scale associated with this coupling (0.18 eV from DF calculations) is much larger than that typical of the Kondo interaction, the total spin of the system is zero and the Kondo resonance is predicted to disappear, in agreement with experiment. Despite the presence of antiferromagnetic rather than ferromagnetic coupling, the latter phenomenon is thus in some sense analogous to the disappearance of the Kondo resonance for Co dimers on an Au(111) surface first observed by Chen *et al* [30].

In conclusion, the Kondo response of Co atoms and dimers adsorbed on or embedded into a Cu(110)(2 × 1)–O surface has been investigated via STM/STS and DF simulations, finding that Co dimers incorporated into adjacent rows of the surface reconstruction show Kondo resonances decoupled from each other, whereas they are antiferromagnetically coupled (and do not exhibit a Kondo effect) when they are aligned on the same row. This shows that it is possible to couple/uncouple single carriers of the Kondo effect via a proper choice of the adsorption and host geometry, an important finding for the understanding and design of strongly correlated electronic devices. Additionally, it is shown that an oxidic environment (thus closer to real-world systems) presents features remarkably different from pure metal substrates, not only because the oxygen atoms can mediate the interactions among impurity atoms, but also because they influence their charge and spin state, and thus ultimately their Kondo response.

This research has been supported within the Advanced Grants of European Research Council (project ‘SEPON’ grant no. ERC-2008-AdG-227457) and by the Rektor of the Karl-Franzens University Graz.

References

- [1] Kondo J 1964 *Prog. Theor. Phys.* **32** 37
Kondo J 1968 *Phys. Rev.* **169** 437
- [2] Hewson A C 1997 *The Kondo Problem to Heavy Fermions* (Cambridge: Cambridge University Press)
- [3] Grüner G and Zawadowski A 1974 *Rep. Prog. Phys.* **37** 1497
- [4] Kouwenhoven L and Glazman L 2001 *Phys. World* **14** 33
- [5] Li J, Schneider W-D, Berndt R and Delley B 1998 *Phys. Rev. Lett.* **80** 2893
- [6] Madhavan V, Chen W, Jamneala T, Crommie M F and Wingreen N S 1998 *Science* **280** 567
- [7] Ternes M, Heinrich A J and Schneider W-D 2009 *J. Phys.: Condens. Matter* **21** 053001
- [8] Fano U 1961 *Phys. Rev.* **124** 1866
- [9] Bergmann G 2008 *Phys. Rev. B* **77** 104401
- [10] Gumbsch A, Barcaro G, Ramsey M G, Surmev S, Fortunelli A and Netzer F P 2010 *Phys. Rev. B* **81** 165420
- [11] Neel N, Kröger J, Berndt R, Wehling T O, Lichtenstein A I and Katsnelson M I 2008 *Phys. Rev. Lett.* **101** 266803
- [12] Manoharan H C, Lutz C P and Eigler D M 2000 *Nature* **403** 512
- [13] Wahl P, Diekhöner L, Schneider M A, Vitali L, Wittich G and Kern K 2004 *Phys. Rev. Lett.* **93** 176603
- [14] Baroni S, Del Corso A, de Gironcoli S and Giannozzi P <http://www.pwscf.org>.
- [15] Vanderbilt D 1990 *Phys. Rev. B* **41** 7892

- [16] Perdew J P, Burke K and Ernzerhof M 1996 *Phys. Rev. Lett.* **77** 3865
- [17] Anisimov V I, Zaanen J and Andersen O K 1991 *Phys. Rev. B* **44** 943
- [18] Wdowik U D and Legut D 2008 *J. Phys. Chem. Solids* **69** 1698
- [19] Knorr N, Schneider M A, Diekhöner L, Wahl P and Kern K 2002 *Phys. Rev. Lett.* **88** 096804
- [20] Újsághy O, Kroha J, Szunyogh L and Zawadowski A 2000 *Phys. Rev. Lett.* **85** 2557
- [21] Lin C-Y, Castro Nieto A H and Jones B A 2006 *Phys. Rev. Lett.* **97** 156102
- [22] Huang P and Carter E A 2008 *Nano Lett.* **8** 1265
- [23] Costi T A, Bergqvist L, Weichselbaum A, von Delft J, Micklitz T, Rosch A, Mavropoulos P, Dederichs P H, Mallet F, Saminadayar L and Bäuerle C 2009 *Phys. Rev. Lett.* **102** 056802
- [24] Lucignano P, Mazzarello R, Smogunov A, Fabrizio M and Tosatti E 2009 *Nat. Mater.* **8** 563
- [25] Gorelov E, Wehling T O, Rubtsov A N, Katsnelson M I and Lichtenstein A I 2009 *Phys. Rev. B* **80** 155132
- [26] Madhavan V, Chen W, Jamneala T, Crommie M F and Wingreen N S 2001 *Phys. Rev. B* **64** 165412
- [27] Plihal M and Gadzuk J W 2001 *Phys. Rev. B* **63** 085404
- [28] Wahl P, Seitsonen A P, Diekhöner L, Schneider M A and Kern K 2009 *New J. Phys.* **11** 113015
- [29] Schrieffer J R and Wolff P A 1966 *Phys. Rev.* **149** 491
- [30] Chen W, Jamneala T, Madhavan V and Crommie M F 1999 *Phys. Rev. B* **60** R8529
- [31] Wahl P, Simon P, Diekhöner L, Stepanyuk V S, Bruno P, Schneider M A and Kern K 2007 *Phys. Rev. Lett.* **98** 056601
- [32] Goodenough J B 1958 *J. Phys. Chem. Solids* **6** 287
- [33] Kanamori J 1959 *J. Phys. Chem. Solids* **10** 87